



Dielectric Properties of PLA-PGA-Chitosan – Hydroxyapatite composites

N. Montañez Supelano^{1*}, A. Sandoval Amador¹, H. Estupiñan Duran², D. Peña Ballesteros³

1. Grupo de Investigaciones en Corrosión, Universidad Industrial de Santander, Santander – Colombia

2. Laboratorio de Biomateriales, Universidad Nacional de Colombia, sede Medellín - Colombia

3. Centro de Materiales y Nanociencias, Universidad Industrial de Santander, Piedecuesta - Colombia

Received 24 Jun 2017,
Revised 22 July 2018,
Accepted 27 July 2018

Keywords

- ✓ Dielectric properties
- ✓ Osteosarcoma cells
- ✓ Composites coating
- ✓ Ti6Al4V
- ✓ EIS

N Montañez Supelano
ing.nerly.montanez@hotmail.com
+57 7 6344000 ext 3520

Abstract

Electrochemical studies applicable to osteosynthesis materials have been conducted to characterize the interface created between the implant surface and the cells, in the complex processes involved in the mechanisms of interaction of the medical device and the surrounding tissue. An electrochemical technique used is electrochemical impedance spectroscopy (EIS), from which it is possible to calculate the permittivity and conductivity of the system under study in a frequency range, which describe the dielectric response of composites or coatings. These parameters (permittivity and conductivity) provide information on the ability to allow movement of the charge carriers and a measure of the polarizability. In this paper a dielectric spectrum of a coating of polylactic acid (PLA), polyglycolic acid (PGA), chitosan and hydroxyapatite (HAp) on discs Ti6Al4V using the EIS technique in a culture medium with human osteosarcoma cells HOS was obtained. According to the obtained spectrum it was evident the dispersions alpha (α) and beta (β) showing the integrity of the biological tissue, related to ion exchange and polarization of the cell membrane. It was found that the best concentration of hydroxyapatite and chitosan interaction osteoblast cell surface modified Ti6Al4V was 15% w/w and 7% w/w Hap and Chitosan respectively in a polymer matrix of PLA-PGA. The surface morphology was assessed by scanning electron microscopy (SEM) and atomic force microscopy (AFM).

1. Introduction

Knowledge of the processes that occur with electrolytic biological media and implantology materials are necessary for the development of materials and their surface modifications in biomaterials. The application of techniques like electrochemical impedance spectroscopy (EIS) to a system, cell – culture medium makes that the load distribution surrounding membrane is scattered, the response of the system is then based on polarization – dispersion of cells altered by an electric field [1, 2]. Charge carriers are mainly ions and the most important source of dipole moment lies in polar molecules of water in tissue and proteinaceous and lipid structures that constitute membranes or cell interfaces. The movement of these charges induces a phenomenon conduction in the material, and the polarization of multiple dipoles, resulting in a relaxation phenomenon or dielectric dispersion. The electrical impedance of a tissue volume in a frequency sweep provides information about the cell population and their electrical properties [3, 4].

Polarization mechanisms and relaxations are defined as dispersions dielectric [5], that in a frequency vs. relative permittivity diagram showing the permittivity decrease with frequency increasing ideally in three steps which are designated dispersions α , β , γ . Dispersion α (below 1×10^3 Hz) is associated with the interfacial

polarisations in the electrical double layer and the effects of ionic conduction in the limits of the biological membrane. Dispersion β (between $1 \times 10^4 - 1 \times 10^5$ Hz), associated with the properties of the cell membrane and its interaction with electrolytes intra and extra cellular and dispersion γ ($> 1 \times 10^6$ Hz) is due to orientation of dipoles and the relaxation of water molecules in the tissue [6, 7]. Biophysical mechanisms responsible for the electrical properties of tissue are associated with the cell membrane and electrolyte status of intra and extra cellular [8].

Furthermore, the bone has several electromechanical properties anisotropic type, which are influenced by the amount of calcium and phosphorus, however remodeling mechanisms have not been fully understood [9].

Understanding of electrochemical processes of the cell - material system allows understanding through data permittivity and conductivity electrical effects on the topography and chemical composition of the sample under analysis [1]. The study of dielectric properties has been of interest for numerous biomedical applications, including bone grafts [10]. The objective of this research was to characterize the system electrically HOS cells on polymer matrix coatings of PLA-PGA-chitosan and ceramic, hydroxyapatite to evaluate the dielectric response (permittivity and conductivity) in the adherence process of the cells under study. EIS technique was used, for getting dielectric measures that allowed to evidence the cell membrane polarization in a dielectric spectrum, parameters involved in healthy tissue and its favorable interaction with the material under study.

2. Experimental details

Ti6Al4V alloy with a size of 12 mm diameter and 3 mm thick was the sample of work. These samples were manual polishing and mechanic with silicon carbide abrasive paper (SiC) grain 400, 600, 800, 1000, 1200 and 1500 until obtain completely homogeneous surfaces.

Polylactic acid (PLA) and polyglycolic acid (PGA) were prepared in previous work with zinc chloride ($ZnCl_2$) as catalyst. Both polymers are characterized by infrared spectroscopy fouriertransformr (FTIR) [11]. Aqueous precipitation method was used to obtain hydroxyapatite, using nitrate tetrahydrate calcium ($Ca(NO_3)_2 \cdot 4H_2O$) and ammonium dihydrogen phosphate ($(NH_4)_2H_2PO_4$). Hydroxyapatite was characterized qualitatively and quantitatively by X-ray diffraction on a powder diffractometer (Bruker geometry DaVinci, D8 Advance, Germany), at a voltage of 40kV, current 30 mA, with internal standard corundum - alumina and sampling of 0.02° (2θ). Cell culture line HOS (human osteosarcoma) it was conducted in RPMI 1640 with 1% L-glutamine, 1% antibiotics [11]. Chitosan was purchased from Sigma Aldrich, of formula $C_{12}H_{24}N_2O_9$, reference 417963-256 CAS9012-76-4, with a degree of deacetylation of 85%, molecular weight 190-275 g/mol.

2.1. Preparation of the polymer matrix

Both polymers powdered dry blended in a proportion of 70% by weight of polylactic acid and 30% by weight of polyglycolic acid, then the mixture was melted at $200^\circ C$ for 20 minutes. This mixture was dissolved in acetone at a concentration of 15% w/v.

The chitosan concentration was 3% and 7% by weight and hydroxyapatite was varied in two points 5 and 15% by weight. Each mixture was carried out in duplicate.

2.2. Electrodeposition

Coating was performed on samples previously treated Ti6Al4V, applying a voltage of 3 volts for a time of 10 minutes, without stirring and at standard pressure and temperature conditions. As anode stainless steel sheet was used. The power source EC570-90 brand Thermo Electron Corporation was used for electrodeposition. Acetone ($CH_3(CO)CH_3$) was used as a solvent.

2.3. Electrochemical impedance spectroscopy

Assays impedance were performed to electrically characterize the HOS cells membrane cultured on polymer coatings. The working electrode (Ti6Al4V) and the counter electrode (Pt wire) were arranged symmetrically to obtain a uniform current distribution. The reference electrode of calomel (Hg/Hg_2Cl_2) sufficiently placed near the surface of the working electrode by a Luggin capillary, to allow compensate the ohmic drop of the solution and will not alter the uniform current distribution as shown in figure 1.

Before measurements EIS, the corrosion potential was recorded for 10 minutes until the potential stabilized. EIS experiments were performed with delta values lower corrosion potential of 5 mV. A sine wave amplitude of 10 mV with a frequency sweep 100000 - 0.01 Hz was applied. The cell culture time on coatings were 0 and 24 h. The cell concentration was 30000 cells / ml, 1ml of cells used in the desired concentration and 4 ml RPMI media.

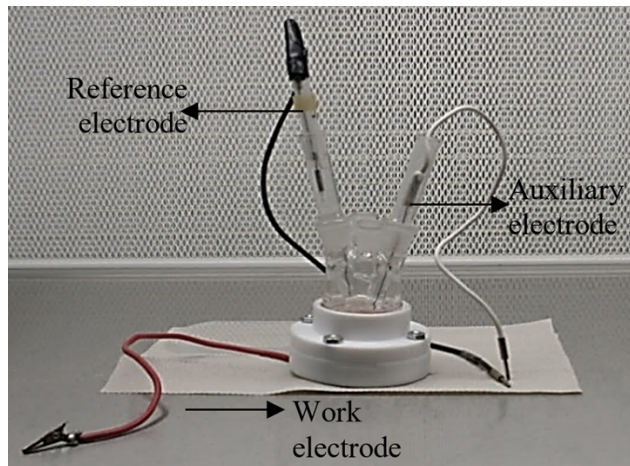


Figure 1. Cell design.

The electrochemical cell was placed in an incubator at 37 °C and 5% CO₂. This system was connected to a potentiostat (Gamry ZRA 600, USA).

To graph the dielectric spectrum equation 4 was used in the calculation of the relative permittivity using impedance data, wherein $\omega = 2\pi f$ is the angular frequency, $C = 1/2\pi fZ''$ is the capacitance, $R = Z'$ is the resistance and $\epsilon_0 = 8,854 \times 10^{-12}$ F/m is the vacuum permittivity. With equation 5 it is possible to calculate the dielectric loss. An AC polarization is assumed and relaxation in a uniform dielectric according to Debye relaxation model (1) [12, 13].

$$\epsilon(\omega) = \epsilon'_{\infty} + \frac{\Delta\epsilon'}{1+j\omega\tau} \quad (1)$$

The characteristic relaxation time constant is $\tau = RC$, ϵ'_{∞} is the value of the permittivity at high frequencies, which is a very low value compared to the permittivity at low frequencies. Equation 1 in quadrature components is (equation 2 and 3) [12]:

$$\epsilon' = \epsilon'_{\infty} + \frac{\Delta\epsilon'}{(1+\omega^2\tau^2)} \quad (2)$$

$$\epsilon'' = \frac{\Delta\epsilon'\tau\omega}{(1+\omega^2\tau^2)} \quad (3)$$

ϵ' y ϵ'' are the relative permittivity and dielectric loss or loss factor respectively.

The loss factor can also be calculated as $\epsilon'' = \sigma'/(\epsilon_0\omega)$, σ' is the conductivity. Rewriting (2) and (3) and considering that in vitro data in tissue $\epsilon' = C$ (model series resistor and capacitor) is obtained [12, 14].

$$\epsilon' = \frac{C}{(1+\omega^2C^2R^2)*\epsilon_0} \quad (4)$$

$$\epsilon'' = \frac{\omega C^2 R}{(1+\omega^2C^2R^2)*\epsilon_0} \quad (5)$$

The real part of the AC conductivity was calculated using equation 3 [15]. Z' is the real impedance and Z'' is the imaginary impedance.

$$\sigma' = \frac{Z'}{Z'^2+Z''^2} \quad (6)$$

2.4. Scanning electron microscopy and atomic force microscopy

For SEM, cells with 50 μ l of methanol are fixed, they allowed to dry at - 4 ° C for 48 hours. Followed, washed with PBS and the procedure for the post-fixing is repeated. Samples for AFM carried to the point of post-fixing. Scanning electron microscopy was performed in a scanning electron microscope FEI Quanta 650 FEG, with an EDAX detector APOLLO X (126.1 eV resolution (Mn K α)) for EDS. The surface characterization by AFM analysis was performed on a computer Auto Probe CP Park SCIENTIFIC INSTRUMENTS signature. Microscopies analysis was done by software WSxM Scanning Probe Microscopy.

3. Results and Discussion

The qualitative analysis of the phases present in the hydroxyapatite was performed by comparing the profile observed with the diffraction profiles reported in the database PDF-2 of the International Centre for Diffraction Data (PDF-2 Number of Hydroxyapatite card 010-74-7080, and whitlockite 000-55-0898), ICDD reference) (figure 2). The presence of crystalline phases of hydroxyapatite is evident in 84.9% and tricalcium phosphate (whitlockite) in 15.1%. The latter presents a lesser extent. Quantitative analysis of the phases found was performed using the Rietveld method refinement Profile I observed when they had added to the internal standard shows a known amount (Aluminum oxide, -100 mesh, 99%, Corundum, α -phase. Aldrich No. 23,474 -5) corresponding to 20%.

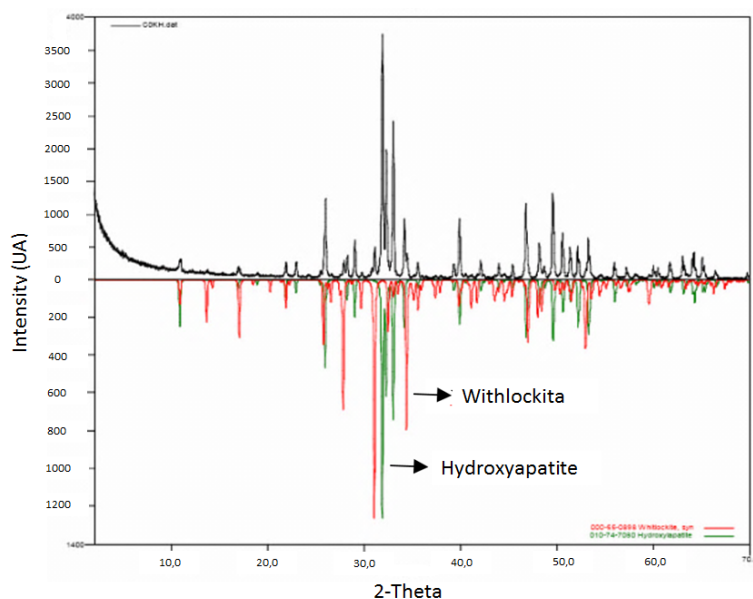


Figure 2. X –ray diffraction of hydroxyapatite.

Applying spectroscopy electrochemical impedance technique is a direct measure of the impedance cell suspension it provides the electric field. Making a frequency sweep allows to find the characteristic spectrum of Bode and Nyquist, where electrical parameters occurring in the media-cells-coating-Ti6Al4V interface at times culture of 0 and 24 hours is determined. Figure 3 shown the Bode diagram and Figure 4 the Nyquist plot at 24 hours incubation for the different mixtures.

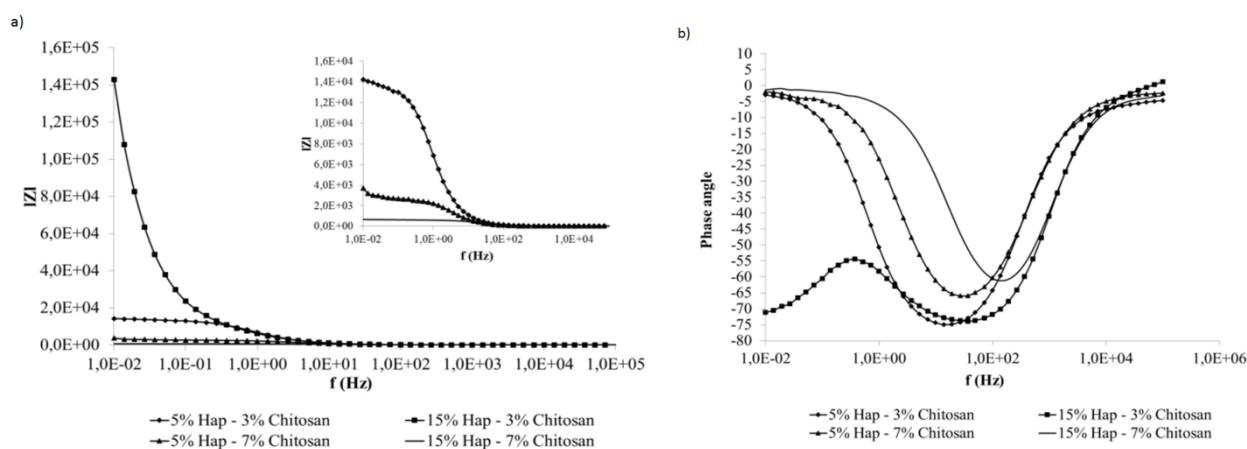


Figure 3. Bode plot for different mixtures HAp – Chitosan, 24 hours incubation HOS. a) Module impedance vs. frequency, b) Phase angle vs. frequency.

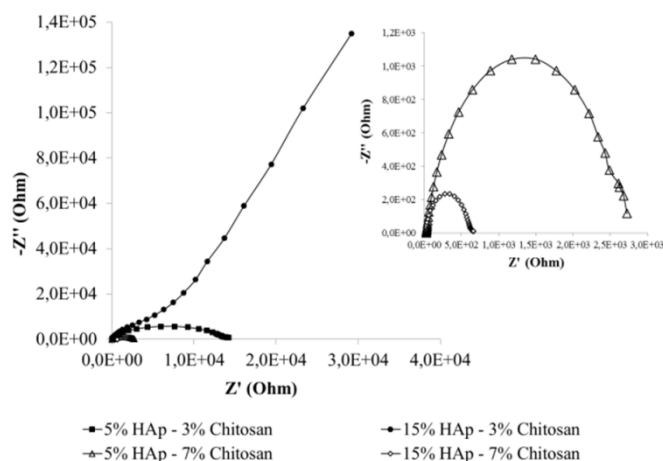


Figure 4. Nyquist plot for different mixtures HAP – Chitosan, 24 hours incubation HOS.

In figure 3a, in the region of medium to low frequencies of 100 a 1×10^{-2} Hz, the impedance module vs frequency showed a change in slope, with a continuous and significant increase in the impedance module, indicating that these frequencies appear processes charge transfer and mass transfer [16] that occur at the interface proteins and biomolecules adsorptive coating [17].

The value of the phase angle high to mid frequency is shown in Figure 3b, decreases from 0° to -75° and medium to low frequencies increases to -1° (taking an average of all mixtures). The decrease in phase angle in presence of osteoblast cells is related to cell adhesion by the proteins forming the extracellular matrix and are absorbed in the polymer-ceramic matrix. Adhesion occurs rapidly and displayed as physical and chemical links between cells and the coating. However, for coating HAp 15% - 3% chitosan is not case, this is because that chitosan acts as an adhesive between the PLA-PGA matrix and hydroxyapatite [18]. Is for this reason that the coating 15% HAp - 7% chitosan has the same tend to other coatings, this trend is dependent on the amount of chitosan contained.

Figure 4 shows the same behavior for coatings except for coating 15% HAp - 3% chitosan, since this coating has a very high impedance. For other coatings the polarization resistance is lower (compared to 0 hours incubation), indicating that the coating-cell system is capacitive and therefore, the cells are in the process of adhesion, being the polymer matrix the support for growth of cells. The coating more capacitive is corresponding to 15% HAp - 7% chitosan evidenced by the Nyquist plot. As can be seen in Figure 5 for coating HAp 5% - 3% chitosan, there was a decrease in the actual impedance comparing 0 hours and 24 hours cell incubation.

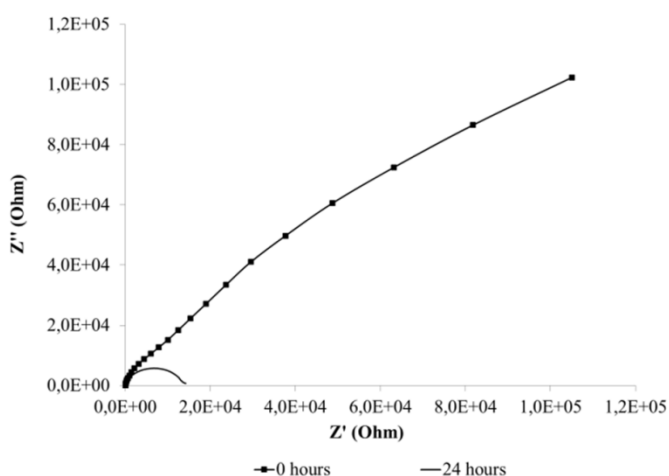


Figure 5. Nyquist plot coating 5% HAp – 3% Chitosan with HOS cells

Figure 6 shows the permittivity and conductivity for different coatings. Figure 6a and 6b follows the characteristics of the Maxwell-Wagner dielectric dispersions. Typical dispersions of a suspension of biological cells in an electrolytic medium are displayed based on interfacial polarization it occurs limits of materials with different electrical properties [1]. The relative permittivity decreases while the conductivity increases, this is the tendency for a normal tissue, demonstrating the integrity of cell membranes in the coating surface [19]. The maximum conductivity and permittivity coating was corresponding to a concentration of HAp and chitosan of 15% and 7% by weight, respectively, followed by coating 15% HAp and 3% chitosan. In Figure 7 the dielectric spectrum is shown for coating and 15% HAp 7% chitosan, which contains the actual permittivity.

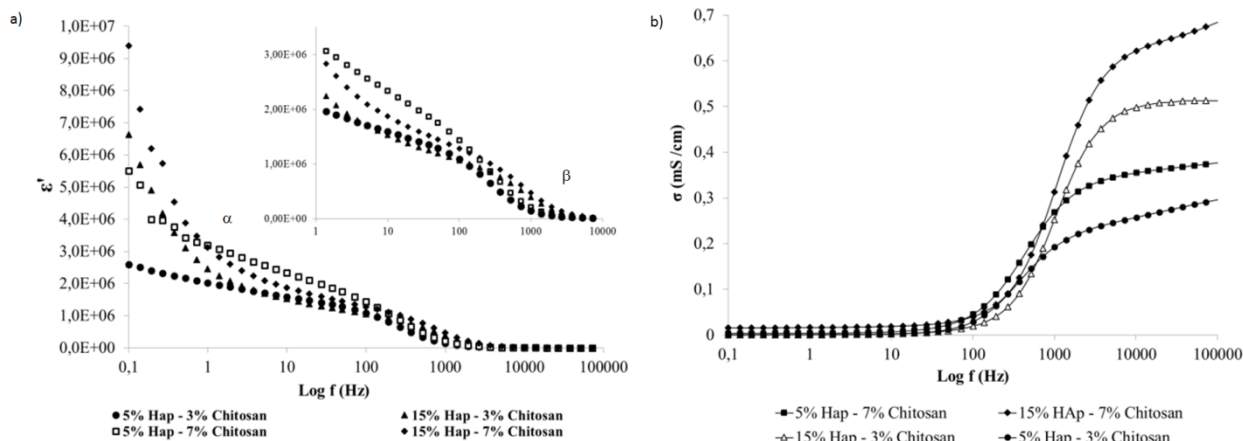


Figure 6. Dielectric spectra Hydroxyapatite(HAp)– Chitosan, 24 hours incubation HOS. a) Relative permittivity, b) Conductivity.

In Figure 7 shows the high values of dielectric loss at low frequencies. This can be explained by the Maxwell-Wagner phenomenon due to the large number of interfaces that constitute the system in study [9]. An isotropic bone tissue has dielectric loss less than an anisotropic tissue. According to the results found of dielectric loss of Saha and Williams, bone tissue is transversely isotropic nature, the results show the anisotropy of the system, that suggest different interfaces to the coating. [20]. Permittivity values for human cortical bone are the order of 1×10^6 at low frequencies (100 Hz), which is consistent with the data presented by Marzec et al [21] and 0,68 mS/cm to frequency 1×10^5 Hz, for the coating of Figure 7, permittivity values are comparable with those of cortical bone [22]. The dielectric spectra found is characteristic of the dielectric spectra of Schwan et al (1962) [12].

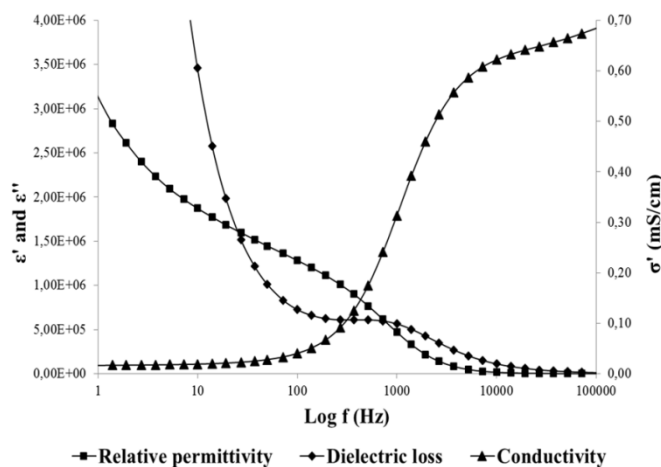


Figure 7. Dielectric spectra. System 15% HAP – 7% Chitosan – HOS cells.

Figure 8 show the SEM for coating 5% HAp – 3% chitosan, it's shows the naked sites where detached coating. Figure 9 shown atomic force microscopies for coatings 5% HAp – 3% chitosan and 15% HAp – 3% chitosan respectively. Less homogeneous surfaces for coatings with higher content of hydroxyapatite and lower content of chitosan are shown in Figure 9, this is due to the integrating effect of chitosan between polymer PLA-PGA and hydroxyapatite. This is consistent with the results found in EIS and the dielectric spectra.

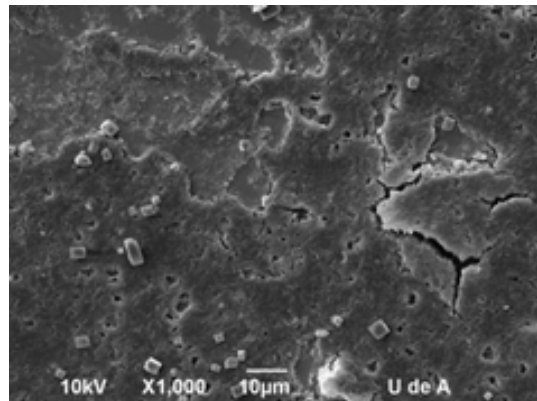


Figure 8. Scanning electron microscopy for coating 5% HAp – 3% Chitosan.

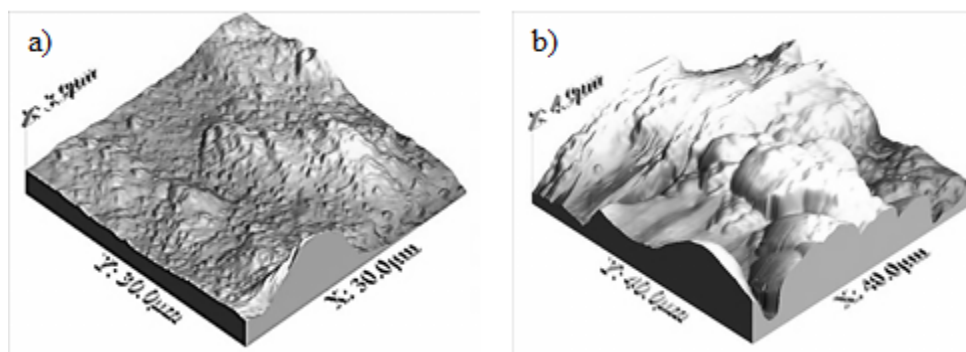


Figure 9. Atomic force microscopy. a) 5% HAp – 3% Chitosan. b) 15% HAp – 3% Chitosan.

Conclusions

A decrease in the resistive component of the electrical impedance in the polymer matrix with hydroxyapatite evidenced, which shows that the cell membranes are capacitive and are in integrity conditions, facilitating the passage of current from the extracellular environment to the intracellular environment, stimulate cell interaction. For all coatings there was a decrease of permittivity achieved observed relaxations alpha and beta according to the frequency sweep corresponding to these relaxations, which correspond to healthy tissue.

Higher permittivity and conductivity values were found for the coating 15% and 7% HAp chitosan respectively, agreeing this analysis with results found in the resistive component of actual impedance diagram vs imaginary impedance. These effects are due to superficial changes that are occurring in the dependent interface of the concentrations used chitosan and hydroxyapatite, where it is evident that the higher the concentration of chitosan, the coating has less degradation, expressed by the diagram impedances and higher permittivity, this is due to the integrating effect of chitosan between PLA-PGA polymer matrix and hydroxyapatite. The addition of these materials to the polymer matrix PLA-PGA favors the growth of osteoblast cells. The material composed of the polymer and the modifying material make this potential for performing orthopedic implants.

Acknowledgments—The authors want to give thanks to Universidad Industrial de Santander, Vicerrectoría de Investigación y Extensión for funding this Project under internal code 1888.

References

1. K. Heileman, J. Daoud y M. Tabrizian, *Biosens. Bioelectron*, 49 (2013) 348–359.
2. A. Ron, I. Shur, R. Daniel, R. Raj, N. Fishelson, N. Croitoru, D. Benayahu y Y. Shacham, *Bioelectrochemistry*, 78 (2010) 161–172.
3. D. Dean, D. Ramanathan, D. Mahado y R. Sundararajan, *J. Electrostat*, 66 (2008) 165–177.
4. M. Moncada, A. Martinez, C. Pinedo y H. Cadavid, *Revista Facultad de Ingeniería Universidad de Antioquia*, 44 (2008) 75-82.
5. I. Ivanov y B. Paarvanova, *Bioelectrochemistry*, 110 (2016) 59-68.
6. R. Pethig, *IEEE transactions on electrical insulation*, 19, 5, (1984) 453-474.
7. E. Gheorghiu, *Bioelectrochem. Bioenerg*, 38 (1995) 123-127.
8. H. Schwan y K. Foster, *Proce IEEE*, 68, 1, (1980) 104-113.
9. I. Ciuchi, L. Curecheriu, C. Ciomaga, A. Sandu y L. Mitoseriu, *J. Adv. Res. Phys*, 1, 1, (2010) 1-5.
10. I. Petrov, O. Kalinkevich, M. Pogorielov, A. Kalinkevich, A. Stanislavov, A. Sklyar, S. Danilchenko y T. Yovcheva, *Carbohydr. Polym*, 151, 20, (2016) 770-778.
11. N. Montañez, M. Gelves, H. Estupiñán, C. Vásquez y D. Peña, *Puente Revista Científica*, 5(2) (2011) 27-32.
12. S. Grimnes y O. Martinsen, *Bioimpedance & Bioelectricity*, Second Edition ed., Great Britain: Elsevier, 2008.
13. K. Cole, *J. Chem. Phys*, 9, (1941) 341-351.
14. H. Coster, T. Chilcott y A. Coster, *Bioelectrochem. Bioenerg*, 40, (1996) 79-98.
15. J. Gittings, C. Bowen, A. Dent, I. Turner y F. Baxt, *Acta Biomater*, 5, 2, (2009) 743-754.
16. A. Balamurugan, G. Balossier, J. Michel y J. Ferreira, *Electrochim. Acta*, 54, (2009) 1192–1198.
17. A. García, L. Saldaña, C. Alonso, V. Barraco, M. Muñoz y M. Escudero, *Acta Biomater*, 5, 4, (2009) 1374–1384.
18. A. Martel, C. Martínez, J. Chacón, P. García y I. Olivas, *Carbohydr. Polym*, 81, 4, (2010) 775-783.
19. O. Casas, «Contribución a la obtención de imágenes paramétricas en tomografía de impedancia eléctrica para la caracterización de tejido biológicos,» Doctoral Thesis. Universidad Politécnica de Catalunya, España, 1999.
20. S. Saha y P. Williams, *Ann. Biomed. Eng*, 17, (1989) 143-158.
21. E. Marzec y W. Warchol, *Bioelectrochemistry*, 65 (2005) 89– 94.
22. C. Gabriel, S. Gabriel y E. Corthout, *Phys. Med. Biol*, 41 (1996) 2231–2249.

(2018) ; <http://www.jmaterenvirosci.com>